

## Hole-tunneling dynamics in biased GaAs/Al<sub>0.35</sub>Ga<sub>0.65</sub>As asymmetric double quantum wells

M. Nido,\* M. G. W. Alexander, and W. W. Rühle

*Max-Planck-Institut für Festkörperforschung, D-7000 Stuttgart 80, Federal Republic of Germany*

K. Köhler

*Fraunhofer-Institut für Angewandte Festkörperphysik, D-7800 Freiburg, Federal Republic of Germany*

(Received 31 August 1990)

Hole tunneling is investigated by picosecond photoluminescence in two biased asymmetric double-quantum-well samples with different hole subband spacing. Spatially indirect excitons are observed above a threshold field. The energy difference between the wide-well direct and the crossed indirect exciton reveals the energy differences between hole subbands. Nonresonant tunneling with fast transfer times occurs above this threshold field without the contribution of optical phonons. Resonances in the hole-tunneling-transfer times occur at higher fields and are ascribed to mixing effects between heavy and light holes in adjacent wells.

Tunneling phenomena of holes in semiconductor heterostructures have been recently investigated theoretically<sup>1-3</sup> as well as experimentally<sup>4-10</sup> mainly by transport measurements. While electron tunneling in such systems has been intensively studied,<sup>11</sup> experiments on hole tunneling are still sparse and infrequent. Furthermore the complicated valence-band structure imposes difficulties on the interpretation. The contribution of heavy- and light-hole mixing effects to hole tunneling in GaAs/Al<sub>x</sub>Ga<sub>1-x</sub>As (Refs. 4-6) is still controversial. Very little is known about the dynamics of this process in general, and about the transfer times in particular. The knowledge of the mechanism and times for hole tunneling is very important for applications, in particular for optoelectronic devices such as effective-mass filtering photodetectors<sup>11</sup> or coupled quantum-well modulators,<sup>12</sup> since both electrons and holes are involved in the device operation. The slowest carrier-transfer time may limit the ultimate device speed in such cases.

Asymmetric-double-quantum-well (ADQW) structures have been introduced in order to investigate tunneling phenomena,<sup>7-10,13-18</sup> since these structures are considered to be ideal to study the physics of tunneling.<sup>19</sup> In particular, time-resolved optical measurements on the ADQW structures are a powerful tool to study the dynamics of tunneling phenomena directly.<sup>7-10,14-18</sup> However, most investigations concentrated on electron tunneling which is considered to be much faster than hole tunneling.<sup>14-18</sup> Only a small number of experiments on hole-tunneling dynamics in the ADQW structures were reported very recently.<sup>7-10</sup>

Norris *et al.*<sup>7</sup> first presented time-resolved photoluminescence (PL) data on charge-transfer states caused by electron and hole tunneling in ADQW's but they did not give absolute values for hole-tunneling-transfer times. Leo *et al.*<sup>8</sup> reported observations of hole tunneling in ADQW's biased with a perpendicular electric field. They observed only resonant hole transfer from the wide-QW ground heavy-hole subband to the narrow-QW second heavy-hole subband and concluded that mixing between heavy and light holes does not lead to more efficient resonant tunneling than between heavy-hole states. We previ-

ously reported observations of hole tunneling in ADQW's with several barrier thicknesses under flat-band conditions<sup>9</sup> as well as with an electric field applied perpendicular to the ADQW's.<sup>10</sup> We demonstrated that the hole-tunneling-transfer times strongly decrease at electric-field values where either the wide-QW ground heavy-hole subband is energetically aligned with the narrow-QW ground light-hole subband or GaAs longitudinal optical (LO)-phonon scattering from the wide-QW to the narrow-QW ground heavy-hole level becomes possible. However, we were not able to distinguish between the two processes because of the QW widths used in our previous work.<sup>10</sup>

In this paper, we present a systematic and unambiguous dynamical investigation of hole tunneling in biased ADQW's, using the direct- and indirect-exciton luminescence<sup>7,20</sup> for calibrating the valence-subband energies. The hole-tunneling-transfer times are measured by picosecond PL. We report absolute values of nonresonant hole-tunneling-transfer times, which are surprisingly fast. Two samples with different hole subband spacing are investigated in order to distinguish the contributions of mixing between heavy and light holes and LO-phonon scattering. The mixing between heavy and light holes in adjacent wells seems to be important for the resonant transfer.

The samples used in our experiments are all grown by molecular-beam epitaxy (MBE) on Si *n*<sup>+</sup>-type doped (100) GaAs substrate. The buffer layer following the substrate has been described in detail previously.<sup>9</sup> Between the buffer and the ADQW, an isolated QW of 10-nm GaAs is grown. This isolated 10-nm QW is used to calibrate the electric field inside the heterostructure, as will be described in detail later. The ADQW structure itself consists of a 100-nm Al<sub>0.35</sub>Ga<sub>0.65</sub>As layer, a wide GaAs QW (QW<sub>w</sub>), a 4-nm Al<sub>0.35</sub>Ga<sub>0.65</sub>As barrier layer, a narrow GaAs QW (QW<sub>n</sub>), and a 100-nm Al<sub>0.35</sub>Ga<sub>0.65</sub>As layer. A 4-nm GaAs cap layer covers the structure. Two samples with different QW<sub>w</sub> and QW<sub>n</sub> thicknesses have been prepared. Sample *A* has a 5-nm QW<sub>w</sub> and a 4-nm QW<sub>n</sub>, and sample *B* has a 4-nm QW<sub>w</sub> and a 3-nm QW<sub>n</sub>. The two samples are designed to have different spacing between the ground heavy- and light-hole subbands. This allows us to distinguish between mixing of heavy and light

holes and LO-phonon scattering. The spacing between the heavy- and light-hole ground states in  $QW_n$  is experimentally determined under flat-band conditions by photoluminescence excitation (PLE) spectroscopy and is 34 meV for sample *A* and 39 meV for sample *B*.

A conventional Ohmic contact of Au-Ge/Ni is alloyed into the substrate side of the samples. Semitransparent 5-nm thick Ni-Cr Schottky contacts of 1.0 mm diameter are evaporated on the front side. The Schottky diodes are reverse biased in the experiments, showing low reverse dark currents  $\leq 5 \mu\text{A}$  and breakdown voltages of more than 6 V. The samples are fixed on a cold finger in a helium cryostat and cooled down to a temperature of 5 K.

Excitation is performed with pulses of about 5 ps width, obtained from a tunable Styryl-8 dye laser, synchronously pumped by a mode-locked Ar<sup>+</sup>-ion laser with a repetition rate of 80 MHz. The PL from the samples is dispersed by a 0.32-m-focal-length monochromator and detected by a two-dimensional synchroscan streak camera with an *S*-20 cathode. The time- and wavelength-resolved PL spectra are thus obtained with a temporal resolution of 6.5 ps and a spectral resolution of 0.5 nm. The excitation density is about  $10^9 \text{ cm}^{-2}$  to avoid space-charge and free-carrier effects. The excitation energy in our experiments is adjusted in such a way that the direct heavy-hole exciton in  $QW_w$  is excited resonantly in order to avoid initial carriers in  $QW_n$  and delays by free-carrier cooling and exciton formation in  $QW_w$ . The PL decay of the direct exciton in  $QW_w$  is fitted by a single-exponential decay giving the decay time constant  $\tau_w^*$ . Hole-tunneling-transfer times can then be obtained using the relation<sup>15</sup>

$$1/\tau_w^* = 1/\tau_R + 1/\tau_T, \quad (1)$$

where  $\tau_R$  and  $\tau_T$  correspond to the direct-exciton radiative-decay time and the hole-tunneling-transfer time out of  $QW_w$ , respectively.

A schematic band structure of the ADQW's is shown in Fig. 1. The first electron subbands in  $QW_w$  and  $QW_n$

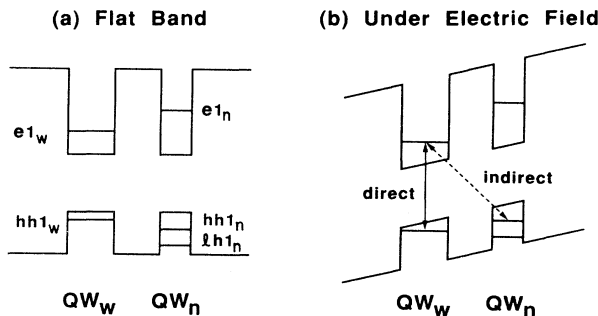


FIG. 1. Schematic drawings of the ADQW band structures. The first electron subbands in  $QW_w$  and  $QW_n$  ( $e1_w$  and  $e1_n$ ), the first heavy-hole subbands in  $QW_w$  and  $QW_n$  ( $hh1_w$  and  $hh1_n$ ), and the first light-hole subband in  $QW_n$  ( $lh1_n$ ) are drawn as solid lines. (a) The figures give the band structures under flat-band conditions and (b) under reverse bias between  $F_1$  and  $F_2$ . In (b), the two exciton transitions observed experimentally are shown: The  $e1_w$ - $hh1_w$  spatially direct transition is depicted by a solid arrow and the spatially indirect  $e1_w$ - $hh1_n$  transition by a dashed arrow.

( $e1_w$  and  $e1_n$ ), the first heavy-hole subbands in  $QW_w$  and  $QW_n$  ( $hh1_w$  and  $hh1_n$ ), and the first light-hole subband in  $QW_n$  ( $lh1_n$ ) are drawn by solid lines. The  $e1_w$  electrons in our experiment remain localized in  $QW_w$ . Under flat-band conditions, shown in Fig. 1(a), the hole energy of  $hh1_w$  is lower than those of  $hh1_n$  and  $lh1_n$ . The energy of  $hh1_w$  becomes higher in energy than that of  $hh1_n$ , as is depicted in Fig. 1(b), above a threshold field  $F_1$ . This threshold is given by  $F_1 = 2/e(E_{hh1_w} - E_{hh1_n})/(d_w + 2d_b + d_n)$ , where  $E_i$  are the subband energies,  $d_w$ ,  $d_b$ , and  $d_n$  are the thicknesses of  $QW_w$ , the barrier, and  $QW_n$ , respectively, and  $e$  is the elementary charge. Tunneling of  $hh1_w$  holes into  $QW_n$  becomes possible at electric fields above  $F_1$ . At a second field  $F_2 = 2/e(E_{hh1_w} - E_{lh1_n})/(d_w + 2d_b + d_n)$ ,  $hh1_w$  and  $lh1_n$  align energetically and resonant tunneling of  $hh1_w$  holes can occur if heavy- and light-hole states mix. Resonances caused by hole scattering from  $hh1_w$  to  $hh1_n$  under participation of LO phonons are also possible in our ADQW configuration. However, these scattering resonances should occur at a *sample-independent* energy separation between  $hh1_w$  and  $hh1_n$  corresponding to the GaAs LO-phonon energy.

Spatially indirect  $e1_w$ - $hh1_n$  exciton PL [dashed arrow in Fig. 1(b)] can be observed in addition to the spatially direct  $e1_w$ - $hh1_w$  exciton [solid arrow in Fig. 1(b)] above  $F_1$ , as shown in Fig. 2(b) for sample *A*. The indirect exciton PL has very long lifetimes of several nanoseconds as expected from the small overlap of electron and hole wave functions,<sup>7</sup> whereas the direct exciton PL has lifetimes of about 300 ps, which is a reasonable value for the  $QW_w$  thicknesses of our samples.

The electric-field strength inside the ADQW structures is measured modeling the PL peak energy shift of the 10-nm QW by the quantum-confined Stark effect<sup>21</sup> (QCSE) using appropriate parameters.<sup>22</sup> The method has been de-

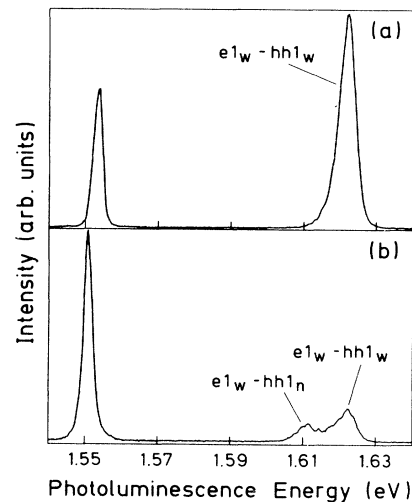


FIG. 2. (a) PL spectra of sample *A* with an electric bias below  $F_1$  and (b) above  $F_1$ . The spectra are taken within the first 200 ps after the excitation pulse. The appearance of the indirect-exciton PL ( $e1_w$ - $hh1_n$ ) in addition to the direct-exciton PL ( $e1_w$ - $hh1_w$ ) can be seen as a split on the right line in (b). The line on the left side is the PL from the isolated 10-nm QW used for the field calibration.

scribed previously in detail.<sup>17</sup> The change in the applied electric field is directly correlated with the change of the subband spacing in the valence band. This is revealed by a separation of the PL peak energies of the direct- and indirect-excitonic recombinations in the ADQW's. The experimentally obtained exciton transition energies are plotted versus the electric field in Fig. 3(a) for sample *A* and Fig. 3(b) for sample *B*. The direct  $e1_w$ - $hh1_w$  and the indirect  $e1_w$ - $hh1_n$  heavy-hole exciton PL energies are depicted by open and solid circles, respectively. The direct-exciton PL energy is almost independent of the electric field for both samples, as expected for thin QW's (Ref. 21) of 5 and 4 nm well widths, whereas the indirect-exciton PL decreases linearly with electric field.<sup>7</sup> Dash-dotted lines and solid lines are least-squares fits for the direct- and the indirect-exciton data points, respectively.

The calculated  $e1_w$ - $lh_n$  indirect exciton PL energies are also shown by dotted lines in Fig. 3. These transition energies can be calculated under two assumptions: First, the energy separation between  $hh1_n$  and  $lh1_n$  does not change significantly with electric field for the small QW's, which are only 4 and 3 nm thick in our case.<sup>21</sup> We therefore assume a field-independent energy separation of 34 and 39 meV for samples *A* and *B*, respectively, as obtained by PLE measurements under flat-band conditions. Second, the difference of the exciton binding energies for heavy- and light-hole excitons can be neglected for indirect excitons, since the absolute values are already small.<sup>20</sup>

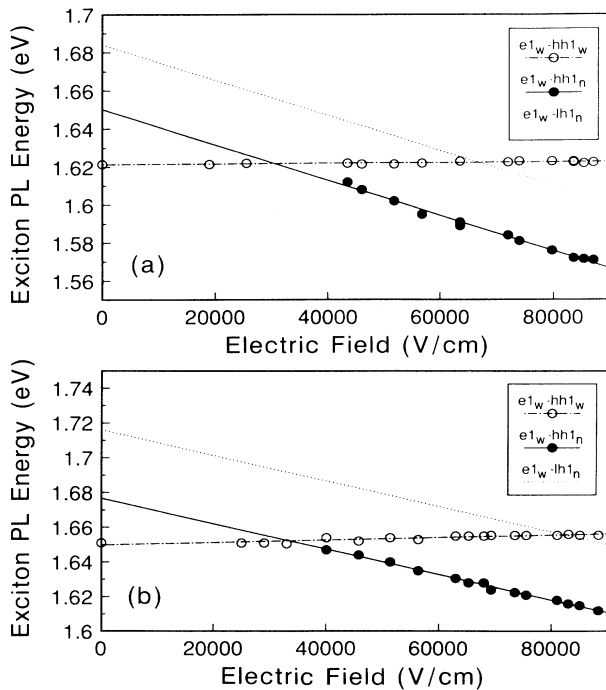


FIG. 3. (a) Exciton PL energies vs electric field for sample *A* and (b) sample *B*. The  $e1_w$ - $hh1_w$  spatially direct-exciton PL energies are plotted by open circles and the  $e1_w$ - $hh1_n$  spatially indirect-exciton PL energies are depicted by solid circles. Dash-dotted and solid lines are least-squares fits to the data points. The dotted lines are the  $e1_w$ - $hh1_n$  spatially indirect-exciton PL energies, calculated as described in the text.

We will now discuss the dynamical features of the hole-tunneling transfer as a function of the subband spacing between  $hh1_w$  and  $hh1_n$ . Figure 4 shows the QW<sub>*n*</sub> direct exciton PL decay times  $\tau_w^*$ , which reveal the transfer times according to Eq. (1), versus the energy difference  $\delta$  between the direct- and the indirect-exciton PL energies. The value of  $\delta$  is a more accurate and direct measure for the energy difference between  $hh1_w$  and  $hh1_n$  than calculating the difference between  $hh1_w$  and  $hh1_n$  from the measured electric field. We therefore use the direct method in this paper whenever possible.<sup>23</sup> In the region of negative  $\delta$ , where the indirect exciton is unobservable, the energy difference is still estimated from the QCSE, i.e., the difference between the dash-dotted and the solid lines in Fig. 3.

Open and solid triangles show the data points for samples *A* and *B*, respectively. Two important features can be clearly seen for both samples: First, in the region where the energy difference is negative, the PL decay times  $\tau_w^*$  have almost constant values determined by the direct-exciton radiative decay. The hole-tunneling-transfer time  $\tau_T$  is infinite, since no tunneling is possible and Eq. (1) gives  $\tau_w^* = \tau_R$ . The PL decay times  $\tau_w^*$  decrease abruptly when  $hh1_w$  and  $hh1_n$  are aligned. For larger fields the times stay almost constant, with about 60 ps for sample *A* and 30 ps for sample *B*, up to the onset of a second decrease. The times become minimal at energy separations  $\delta$  with *sample-dependent* values of 34 meV for sample *A* and 40 meV for sample *B*. The decay times  $\tau_w^*$  slightly increase again beyond these resonances.

The flat region between the two decreases is the nonresonant-tunneling regime with tunneling-transfer times almost independent of  $\delta$ . In the case of nonresonant hole tunneling, the hole momentum parallel to the QW interfaces must change. Some scattering process must induce this change, which could be LO-phonon scattering, impurity or interface-defect scattering, scattering at interface roughness, or alloy scattering. The onset of nonresonant hole tunneling when  $hh1_w$  and  $hh1_n$  are aligned and the

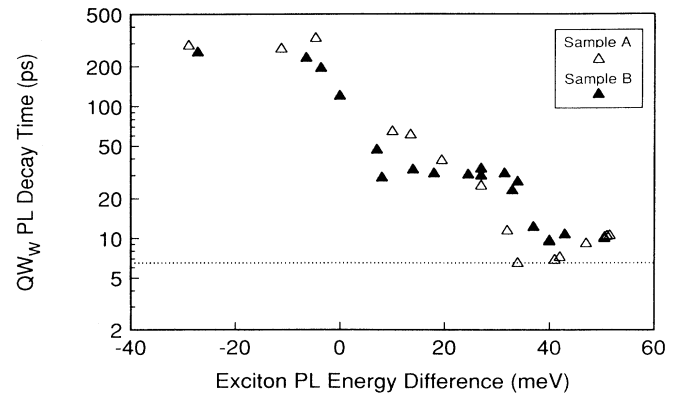


FIG. 4. Decay times of the  $e1_w$ - $hh1_w$  exciton PL  $\tau_w^*$  vs the PL energy difference  $\delta$  between the  $e1_w$ - $hh1_w$  and  $e1_w$ - $hh1_n$  excitons. Open and solid triangles depict data points for sample *A* and *B*, respectively. The dotted line represents our time resolution.

almost constant transfer times for an energy difference  $\delta$  up to 30 meV demonstrates that efficient and surprisingly fast nonresonant hole tunneling can happen *without* LO-phonon participation.

Resonances are observed when the energy difference  $\delta$  is 34 meV for sample *A* and 40 meV for sample *B*. At the electric fields where the  $e1_w$ - $hh1_w$  and  $e1_w$ - $lh1_n$  exciton PL energies are equal, the energy differences between the  $e1_w$ - $hh1_w$  and  $e1_w$ - $lh1_n$  exciton PL energies are 34 and 39 meV for sample *A* and *B*, respectively (see Fig. 3). These energy differences coincide very well with the observed energy differences at the minima in Fig. 4, which leads us to the assumption that the observed resonances are  $hh1_w$ - $lh1_n$  transitions. It is unlikely that these resonances are due to the onset of LO-phonon scattering from  $hh1_w$  to  $hh1_n$ , since the energy difference  $\delta$  at the resonance minima would be the same for both samples in that case. Therefore, mixing effects between heavy and light holes, which have been already predicted theoretically<sup>2,3</sup> and observed experimentally,<sup>5,6</sup> seem to be the reason for the hole-tunneling resonances in our experiment. It should be noted, however, that we can neglect heavy holes with initially excited finite parallel momentum since we excite resonantly the  $e1_w$ - $hh1_w$  exciton at a temperature of 5 K. We have to conclude that resonant hole tunneling due to heavy- and light-hole mixing is effective even at these excitation conditions. Further investigations are necessary to clarify this point.

Finally, it is interesting to mention the excitonic character of the tunneling processes in our experiments. Since we excite resonantly the  $e1_w$ - $hh1_w$  exciton and observe

the exciton PL decay times, it is unambiguous that all carriers are bound into excitons before as well as after the transfer process. Changes in the transfer dynamics are found where the direct- and indirect-exciton PL energies become equal. This observation suggests that resonant tunneling of excitonic bound carriers is the transition process from spatially direct to indirect excitons.

In summary, hole-tunneling-transfer processes in ADQW structures biased with a perpendicular electric field are investigated by picosecond PL. Both nonresonant- and resonant-hole-tunneling processes are clearly observed and absolute values of the transfer times are given. The energy difference between the wide QW and the narrow QW heavy-hole subbands is directly determined by detecting the energy difference between the spatially direct- and indirect-exciton PL energies. The nonresonant-tunneling-transfer times are 60 and 30 ps for a 4-nm  $\text{Al}_{0.35}\text{Ga}_{0.65}\text{As}$  barrier for sample *A* and *B*, respectively, without LO-phonon participation. Resonant tunneling seems to happen between the wide-QW ground heavy-hole and the narrow-QW ground light-hole subbands, indicating that mixing effects are important for resonant hole tunneling in  $\text{GaAs}/\text{Al}_x\text{Ga}_{1-x}\text{As}$  structures.

The authors thank M. Altarelli, H. T. Grahn, J. Kuhl, H.-J. Queisser, and R. Wessel for many fruitful discussions. We are indebted to K. Rother and H. Klann for expert technical assistance. Financial support by the Bundesministerium für Forschung und Technologie is acknowledged. One of us (M.N.) thanks M. Sakaguchi and T. Suzuki, NEC Corporation, Japan, for their support.

\*Present address: Opto-Electronics Research Laboratories, NEC Corporation, 4-1-1 Miyazaki, Miyamae-ku, Kawasaki, Kanagawa 213, Japan.

<sup>1</sup>J.-B. Xia, Phys. Rev. B **38**, 8365 (1988).

<sup>2</sup>R. Wessel and M. Altarelli, Phys. Rev. B **39**, 12802 (1989).

<sup>3</sup>E. T. Yu, M. K. Jackson, and T. C. McGill, Appl. Phys. Lett. **55**, 744 (1989).

<sup>4</sup>E. E. Mendez, W. I. Wang, B. Ricco, and L. Esaki, Appl. Phys. Lett. **47**, 415 (1985).

<sup>5</sup>M. K. Jackson, M. B. Johnson, D. H. Chow, and T. C. McGill, Appl. Phys. Lett. **54**, 552 (1989).

<sup>6</sup>H. Schneider, H. T. Grahn, K. v. Klitzing, and K. Ploog, Phys. Rev. B **40**, 10040 (1989).

<sup>7</sup>T. B. Norris, N. Vodjdani, B. Vinter, C. Weisbuch, and G. A. Mourou, Phys. Rev. B **40**, 1392 (1989).

<sup>8</sup>K. Leo, J. Shah, J. P. Gordon, T. C. Damen, D. A. B. Miller, C. W. Tu, J. E. Cunningham, and J. E. Henry, Phys. Rev. B **42**, 7065 (1990).

<sup>9</sup>M. Nido, M. G. W. Alexander, W. W. Rühle, T. Schweizer, and K. Köhler, Appl. Phys. Lett. **56**, 355 (1990).

<sup>10</sup>M. Nido, M. G. W. Alexander, W. W. Rühle, and K. Köhler, in *Applications of Ultrashort Laser Pulses in Science and Technology*, edited by A. Antonetti, SPIE Conference Proceedings No. 1268 (International Society for Optical Engineering, Bellingham, WA, 1990), p. 177.

<sup>11</sup>F. Capasso, K. Mohammed, and A. Y. Cho, IEEE J. Quantum Electron. **QE-22**, 1853 (1986), and references therein.

<sup>12</sup>J. Khurgin, Appl. Phys. Lett. **53**, 779 (1988).

<sup>13</sup>H. W. Liu, R. Ferreira, G. Bastard, C. Delalande, J. F. Palmier, and B. Etienne, Appl. Phys. Lett. **54**, 2082 (1989).

<sup>14</sup>D. Y. Oberli, J. Shah, T. C. Damen, C. W. Tu, T. Y. Chang,

D. A. B. Miller, J. E. Henry, R. F. Kopf, N. Sauer, and A. E. DiGiovanni, Phys. Rev. B **40**, 3028 (1989).

<sup>15</sup>M. G. W. Alexander, W. W. Rühle, R. Sauer, and W. T. Tsang, Appl. Phys. Lett. **55**, 885 (1989).

<sup>16</sup>B. Deveaud, F. Clérot, A. Chomette, A. Regreny, R. Ferreira, G. Bastard, and B. Sermage, Europhys. Lett. **11**, 367 (1990).

<sup>17</sup>M. G. W. Alexander, M. Nido, W. W. Rühle, and K. Köhler, Phys. Rev. B **41**, 12295 (1990).

<sup>18</sup>K. Leo, J. Shah, E. O. Göbel, T. C. Damen, K. Köhler, and P. Ganser, Appl. Phys. Lett. **56**, 2031 (1990).

<sup>19</sup>S. Luryi, Solid State Commun. **65**, 787 (1988).

<sup>20</sup>J. E. Golub, P. F. Liao, D. J. Eilenberger, J. P. Harbison, and T. L. Florez, Solid State Commun. **72**, 735 (1989).

<sup>21</sup>D. A. B. Miller, D. S. Chemla, T. C. Damen, A. C. Gossard, W. Wiegmann, T. H. Wood, and C. A. Burrus, Phys. Rev. B **32**, 1043 (1985).

<sup>22</sup>The parameters for the calculation are effective electron and heavy-hole masses of  $0.067m_e$  and  $0.34m_e$  in the wells and  $0.096m_e$  and  $0.364m_e$  in the barriers, respectively, conduction- and valence-band offsets of 0.289 and 0.156 eV, a band gap for GaAs of 1.519 eV and an exciton binding energy of 0.010 eV. The well widths are fitted, with 95 Å for sample *A* and 92 Å for sample *B*.

<sup>23</sup>It should be noticed that the exciton PL energy difference is not *exactly* the same as the energy spacing between  $hh1_w$  and  $hh1_n$ . The difference between the direct- and indirect-exciton binding energies must be taken into account for an exact correspondence; J. E. Golub, P. F. Liao, D. J. Eilenberger, J. P. Harbison, and T. L. Florez, Solid State Commun. **72**, 735 (1989).